

Numerical Study for Darrieus Turbine with Wind Lens: Performance and Aeroacoustic Analogies

R. A. Ghazalla¹, M. H. Mohamed², A. A. Hafiz³

¹Mechanical Power Engineering Dept., Higher Technological Institute 10th of Ramadan City, Egypt, P.O. Box: 228

^{2,3}Mechanical Power Engineering Dept., Faculty of Engineering e Mattaria, Helwan University, P.O. 11718, Cairo, Egypt

²Mechanical Engineering Dept., College of Engineering and Islamic Architecture, Umm Al-Qura University, P.O. 5555, Makkah, Kingdom Saudi Arabia

(¹eng.radwaa@gmail.com, ²moh75202@yahoo.de, ³aidaahafiz2@gmail.com)

Abstract- Darrieus turbines are gained significant attention especially at domestic zones that is characterized by the low wind speed. The current study is aimed to investigate the aerodynamic performance of Darrieus turbine enclosed by energy conversion system called wind lens. Then a comparison between original aerofoil and the new J-cut profile is done for S1046 symmetric aerofoil. The commercial software ANSYS-Fluent 15.0 is used for all analysis and simulations executed in present work. In the CFD sequence, Unsteady Reynolds-Averaged Navier-Stokes equations (URANS) are resolved using the SIMPLE algorithm for pressure-velocity coupling. Discretization is executed using the Finite-Volume method with second order upwind scheme for all variables. Sequentially an aero-acoustic analogy is performed on the basis of "Ffowcs Williams Hawkins formula". Noise sources are immersed in the fluid at rest. The noise propagation emanated from the sources is solved by wave equation analytically. The results revealed that J-cut profile without wind lens has noticeable effect on the enhancement of power coefficients. Moreover it is generated the least noise intensity. The power coefficient is enhanced by a factor of 1.74 in case of the original S1046 aerofoil enclosed by wind lens and by a factor 1.35 in case of new J-cut profile enclosed by wind lens compared to open turbine.

Keywords- Darrieus Turbine, Aerofoil Shape, Wind-Lens, CFD, Aero-Acoustic

I. INTRODUCTION

The high demand on energy is creeping up every day due to several factors. The depletion of the fossil energy sources are making them more expensive. Besides the aggravation of the global climate change crisis is increased. The whole scenarios are pushing the world towards the dependency on alternative sources of energy. Wind energy is the most promising source among the other sources of renewable energy. Wind energy has the potential to resolve the power demand of the entire world if it can be converted into electricity efficiently. Wind energy is harvested using two categories of modern wind turbines classified according to their axis of rotation namely, Horizontal

Axis Wind Turbine (HAWT) and Vertical Axis Wind Turbine (VAWT). The most famous types of VAWTs are: (a) Savonius type (drag type) invented by Finnish engineer S.J. Savonius in 1922. The rotation speed of Savonius wind turbine is lower than wind speed therefore; it has Tip Speed Ratio (TSR) of 1 or below. (b) Darrieus type (lift type) is patented firstly in France (1925) and in U.S. (1931) by Georges Jean-Marie Darrieus. There are two types for Darrieus VAWTs, namely Eggbeater Darrieus rotor and H-Darrieus (H-rotor) as shown in Fig.1. Darrieus wind turbine can rotate in higher speeds than wind speed so the TSR is greater than 1, but it generates less torque compared to Savonius.

In the last decade VAWTs take more attention from the researchers as it works well in domestic areas. The turbine blades are oriented in Omnidirectional that is suitable for domestic region where the wind direction is frequently changing among the year. VAWTs are suitable for electricity generation due to its quiet behavior which is more suitable for highly populated places. The cost of complex structure of HAWT blades that should be twisted and tapered for optimum performance is higher than the simpler VAWT blades. The stalling behavior it can withstand gust wind, makes it much safer during those weather conditions.

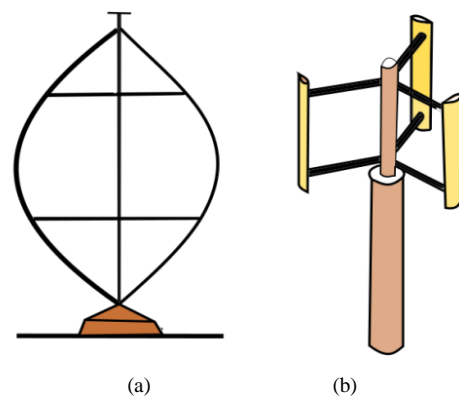


Figure 1. a) Egg beater, b) Three blades H-rotor

VAWT is an appropriate turbine that can be installed in densely populated urban area, away from the main distribution lines and places where large wind farms cannot be installed due to environmental concerns. The main drawbacks of Darrieus turbine is its low performance at built and domestic areas. Therefore, many researchers tried to characterize the most convenient principles of operation to improve the performance of Darrieus turbines, through both experiments and numerical computational methods.

Howell et al. [1] experimented on small scale Darrieus rotor. The experimental study in wind tunnel and computational study was done to find the aerodynamics and performance by changing wind velocity, tip-speed ratio, solidity and rotor blade surface finish. It was concluded that, below a critical wind speed (Reynolds number of 30,000) a smooth rotor surface finish degraded the performance of the turbine. The tests also showed that both two and three bladed rotor models had produced highest performance coefficient, but the three bladed models are more efficient at a much reduced Tip Speed Ratio. Beri and Yao [2] studied the effect of camber airfoil for a self-starting Darrieus turbine. They tested three bladed NACA 2415 camber airfoil at different tip speed ratios. The experimental results showed that, camber airfoil have the characteristics of self-starting. Castelli et al. [3] presented 2-D numerical model simulations using NACA 0021 three bladed rotors with a constant wind speed of 9 m/s to investigate the aerodynamic performance of a straight-bladed Darrieus turbine. Wakui, et al. [4] used hybrid configuration of Darrieus lift type with Savonius drag-type rotors. The result showed that Savonius rotor inside the Darrieus rotor had fine operating behavior to wind speed changes and could be compactly designed because of a shorter rotational axis. This is an effective way for stand-alone small scale systems.

Gupta et al. [5] has compared one simple Savonius and the other combined Savonius– Darrieus wind rotors. The Savonius rotor was a three-bucket system having provisions for overlap variations. The Savonius–Darrieus rotor was a combination of three-bucket Savonius and three-bladed Darrieus rotors with the Savonius placed on top of the Darrieus rotor. This comparative study showed that, there had been a definite improvement in the power coefficient for the combined Savonius–Darrieus rotor without overlap condition. Combined rotor without overlap condition provided an efficiency of 0.51, which was higher than the efficiency of the Savonius rotor at any overlap positions under the same test conditions.

Consult et al. [6] also used a 2D CFD model to determine the effects of varying solidity on VAWT aerodynamic performance at steady inflow. These works proved that the CFD method achieves considerable improvements in the understanding of the basic physics behind VAWTs, and it can be used as an alternative to costly wind tunnel tests.

Mohamed [7] improved the aerodynamic performance of Darrieus turbine (H-rotor) by using 20 different airfoils (non-symmetric and symmetric) in order to maximize output power and output torque coefficients. The results showed that S1046 airfoil is the most promised sectional profile for Darrieus rotor by comparing it with the other profiles considered in this work.

Kanyako and Janajreh [8] examined numerically the performance of a two-dimensional straight three blades Darrieus turbine using different airfoils to get the torque and power output performance. DU-06-W-200, NACA 0015, NACA 0018 and S1046 airfoils are investigated in this work and the results indicated that NACA 0015 is the best performing airfoil for tip speed ratio range from 1 to 4. Since wind power production is proportional to the cubed wind speed which means that the wind velocity plays an important role in power generation. Therefore, notable improvement in output power can be obtained. Accordingly Watanabe et al. [9] experimentally utilized a campaign of wind tunnel experiments to test the effect of applying a wind acceleration device to vertical axis wind turbines. Many optimum parameters affecting the turbine performance were examined. For instant, wind-lens configuration, flange width, semi-open angle, diffuser length, usage of inlet, and wind-lens location. NACA0012, NACA0018, NACA0024, and NACA0030 are examined and the results showed that NACA0024 is the most suitable type in case of using a wind-lens. Ohya et al. [10] provided a unique wind power system that consists of a diffuser equipped with a broad-ring flange attached at the exit periphery and a wind turbine located inside it. This wind acceleration device “wind-lens” is used to augment the output power by collecting and accelerating the wind approaching a wind turbine. Hashem and Mohamed [11] investigated numerically a three-bladed Darrieus turbine using S1046 airfoils equipped with a cycloidal surface diffuser. The results showed that the design has the potential in increasing the power coefficient and it is the most efficient design than using flat or curved diffuser. The main purpose in the present work is to enhance the performance of Darrieus turbine using wind-lens. A different approach is used based on different previous works cited herein. First of all an accurate CFD model is built to describe the basis of developing an accurate 2D transition model of H-rotor and investigating the main parameters affecting such turbine. The model is validated through comparison with experimental wind tunnel results performed by Bravo et al. [12]. A second verification is performed by comparison with another published numerical model for a different case. Noise means spontaneous fluctuations of sound wave received by human ear. The average human hearing range is from 20 Hz to 20 kHz. Two majors noise sources are found in WT the mechanical noise emanated from gear box, auxiliary hydraulic equipment and generator and the aerodynamic noise that the present work concerning about it. This type is formed due to collide of the air over solid bodies such as blades, shaft and wind lens. There is a lack of data on studying of the noise emissions. Iida and Fukudome [13] numerically investigated the sound generated from the VAWT. They concluded that at the HAWT generates more noise than the VAWT at the same normal operating speed. Pearson and Graham [14] are studied the main sources of the noise generation from the VAWT through acoustic investigations methods. They concluded that the harmonics were more vigorous at low tip speed ratio than at higher tip speed ratio due to unsteadiness behavior during the dynamic stall region. Mohamed HM [15] is numerically studied different parameters to decrease the noise generated from Darrieus turbine. He

concluded that the noise increased at high tip speed ratio and high solidity wind turbines.

The noise analysis is a focus of attention in order to install clean renewable devices that didn't impact negatively the environment. The present work aims to fill the gap of lack of data and poor research area that relates with aerodynamic and aero-acoustics of Darrieus turbine.

II. METHODOLOGY AND CODE VALIDATION

The geometrical details of the three straight-bladed Darrieus wind turbine under investigation were summarized in Table [1]. Generating the two-dimensional (2D) VAWT computational domain, meshing, setting the turbulence model and defining its specifications are all achieved by using commercial software ANSYS-Fluent 15.0. The present numerical model contains two main domains; the rotating inner domain and the stationary domain at the outer and in the middle of the rotating domain. The sub-domains are connected via a sliding mesh interface boundary, to ensure the continuity in the flow field. The rotor domain characterized by a moving mesh has three symmetric airfoil blades located on an azimuth angle of 120° relative to each other as shown in "Fig.2" with non-slip rotating wall as boundary condition. The zero pitch angle is the optimal configuration as concluded by Mohamed et al. [16]. Every blade profile inside the rotating domain is enclosed in a control circle called individual domain. Unlike the interface, it has no physical significance but its only aim is to refine the mesh around the airfoil blades.

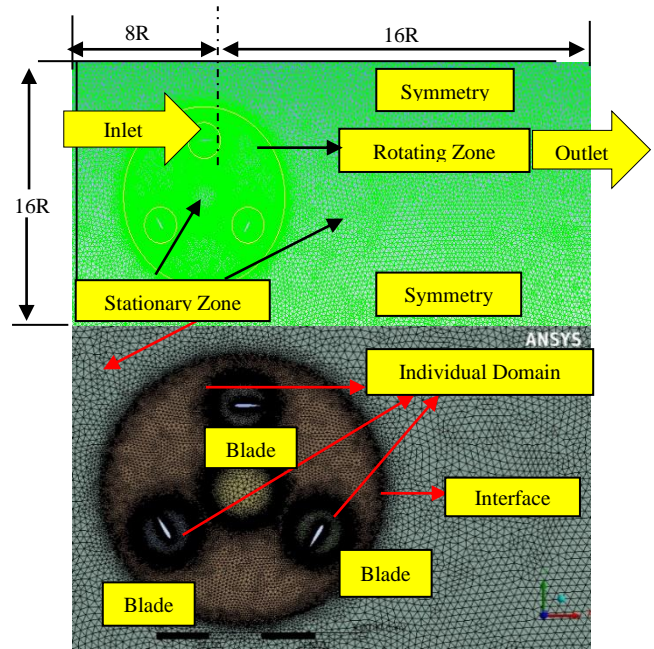


Figure 2. Tri-Unstructured grid (close up view)

The boundary conditions are uniform velocity inlet, zero gauge pressure outlet, symmetry sides and no slip walls (see Table 2). The turbulent length scale at the domain inlet and outlet is selected based on length scale of the turbine diameter. Pressure-velocity coupling is achieved with the SIMPLE (Semi-Implicit Method for Pressure Linked Equations) algorithm, in order to allow faster convergences. Gradient in spatial discretization of least squares cell-Based was used to ensure more accurate results. The second order scheme is used for pressure calculations. Second-order discretization is chosen for momentum equations and turbulence equations including turbulent dissipation rate and turbulent kinetic energy equations are discretized using finite volume method with second-order upwind scheme. For time integration, the second order implicit formulation is used. The continuity equation for unsteady incompressible flow and momentum equations can be calculated in tensorial form as:

$$\frac{\partial u_i}{\partial t} + \frac{\partial u_i}{\partial x_i} = 0 \quad (1)$$

$$\frac{\partial u_i}{\partial t} + u_i \frac{\partial u_i}{\partial x_j} = -\frac{1}{\rho} \frac{\partial p}{\partial x_i} - \frac{\partial}{\partial x_j} \left[\nu \left(\frac{\partial u_i}{\partial x_j} + \frac{\partial u_j}{\partial x_i} - \frac{2}{3} \delta_{ij} \frac{\partial u_k}{\partial x_k} \right) \right] + \frac{\partial}{\partial x_j} (-\tilde{u}_i \tilde{u}_j) \quad (2)$$

Grid independence is checked by successively refining mesh dimensions until negligible changes in the power coefficient at optimum tip speed ratio are obtained see Fig.3. It is concluded that the 807,580 elements is sufficient to ensure that the results are independent to grid size at a moderate computational cost. The grid of 807,580 elements is retained for all further simulations related to open Darrieus turbine paying attention that the number of elements will slightly increase after augmentation of Darrieus turbine with wind-lens.

TABLE I. THE MAIN CHARACTERISTICS OF THE DARRIEUS TURBINE

Parameter	Dimension
Blade profile	NACA 0015
Number of blades N	3
Blade chord length C	0.4 m
Rotor radius R	1.25 m
Rotor height h Turbine area A	1 m (2-D simulation) (2R × H)
Rotor solidity $\sigma = \frac{NC}{2R}$	0.48
Tip speed ratio λ	0.468-1.890
Wind speed U_∞	8 m/s

A rectangular flow domain with mentioned dimensions is adopted as shown in Fig.2. Unstructured triangular mesh is used for both fixed and rotating grids, in order to reduce cost time while preparing CFD simulations. The grid transition on each side of the grid interface has nearly the same element size to avoid divergence phenomena of the model and achieving faster convergence. Intensify the meshing using 20 boundary layers with growth rate 1.2 as near as possible from the wall surface of the turbine blades to capture the viscous sub-layer guaranteed that the maximum value of $Y^+ < 1$. Once the grid is generated, the unsteady two-dimensional Navier Stokes equations are solved using a RANS approximation.

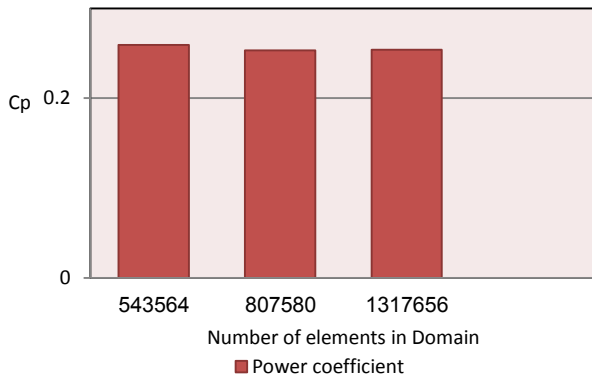


Figure 3. Variation of power coefficient with grid size at $\lambda=1.6$ for open Darrieus turbine.

TABLE II. GRID AND BOUNDARY CONDITIONS.

Parameters	Description
Flow domain	Rectangular(16Rx24R)
Interface type	Sliding/Conformal
Grid type	Unstructured/triangular
Fluid	Air
Turbulence model	K- ω SST
Inlet	Velocity
Outlet	Pressure outlet
Shaft	No-slip moving wall
Blades	No-slip moving wall
Diffuser	No-slip stationary wall
Side	Symmetry
Residual	1×10^{-5}

The SST k- ω turbulence model is selected for CFD simulations in the present study. The SST k- ω model is similar to the k- ϵ turbulence model, but instead of ϵ as the second variable, it uses a turbulence frequency variable ω , which is expressed as $\omega = \epsilon/k$ [s⁻¹]. SST k- ω model calculates Reynolds stresses in the same way as in the k- ϵ model.

The transport equation for turbulent kinetic energy k for the k- ω model is:

$$\frac{\partial(\rho k)}{\partial t} + \frac{\partial}{\partial x_i}(\rho U_i k) = \frac{\partial}{\partial x_i} \left[\left(\mu + \frac{\mu_t}{\sigma_k} \right) \text{grad}(k) \right] + P_k - \beta^* \rho k \omega \quad (3)$$

(I) (II) (III) (IV) (V)

$$\text{where } P_k = \left(2\mu_t \frac{\partial U_i}{\partial x_j} \cdot \frac{\partial U_i}{\partial x_j} - \frac{2}{3} \rho k \frac{\partial U_i}{\partial x_j} \delta_{ij} \right)$$

The terms (I)-(V) in Equation 3, can be defined as the following:

TABLE III. THE TERMS (I)-(V)

(I)	Transient ter	Accumulation of k (rate of change of k)
(II)	Convective transport	Transport of k by convection
(III)	Diffusive transport	Turbulent diffusion transport of k
(IV)	Production term	Rate of production of k
(V)	Dissipation	Rate of dissipation of k

Where, σ, β and γ are equation constants

The transport equation for turbulent frequency ω for the k- ω model is:

$$\frac{\partial \rho \omega}{\partial t} + \frac{\partial}{\partial x_i}(\rho U_i \omega) = \frac{\partial}{\partial x_i} \left[\left(\mu + \frac{\mu_t}{\sigma_{\omega,1}} \right) \text{grad}(\omega) \right] + \gamma_2 \left(2\rho \frac{\partial U_i}{\partial x_j} \cdot \frac{\partial U_i}{\partial x_j} - \frac{2}{3} \rho \omega \frac{\partial U_i}{\partial x_j} \delta_{ij} \right) - \beta_2 \rho \omega^2 + 2 \frac{\rho}{\sigma_{\omega,2}} \frac{\partial k}{\partial x_k} \frac{\partial \omega}{\partial x_k} \quad (4)$$

(I) (II) (III) (IV) (V) (VI)

The general description for each of the terms in Equation 4 (I) to (V) are the usual terms for accumulation, convection, diffusion, production, and dissipation of ω . Last term (VI) is called a ‘cross-diffusion’ term, an additional source term, and has a role in the transition of the modelling from ϵ to ω .

To obtain the torque and power coefficients the following equations are used:

$$C_m = \frac{T}{0.5 \rho A R U \infty^2} \quad (5)$$

$$C_p = \frac{P}{0.5 \rho A U \infty^3} \quad (6)$$

Where, c_m and c_p are the instantaneous torque coefficient and power coefficient respectively.

The built program is validated against an experimental data by Bravo et al. [12] and other numerical data by Lanzafame et al [17] that used SST k- ω see Fig.4 The comparison of C_p of turbine made at different range $0.46875 \leq \lambda \leq 1.875$ are presented to confirm that the present work results were almost in a good acclimation. The comparison reveals same trend for both results having maximum power coefficient at TSR=1.6 for both numerical and experimental data.

Verification is performed as another check for the present model with CFD model introduced by M. Zamani et al. [18]. It is achieved using 3 bladed wind turbine of DU 06-W-200 with chord length 0.27, diameter turbine 3.7 m, shaft radius 0.0575m and wind speed 10 m/s using the k- ω SST turbulence model. The values of C_p obtained at different tip speed ratios $0.10 \leq \lambda \leq 3.50$ are illustrated in Fig. 5 It is clear from the curve that the present CFD model almost congruent with Zamani especially at $\lambda = 2.25$ the $C_p = 0.46$ that is considered as sufficient evidence that the computed power coefficients are in good agreement with obtained computational data.

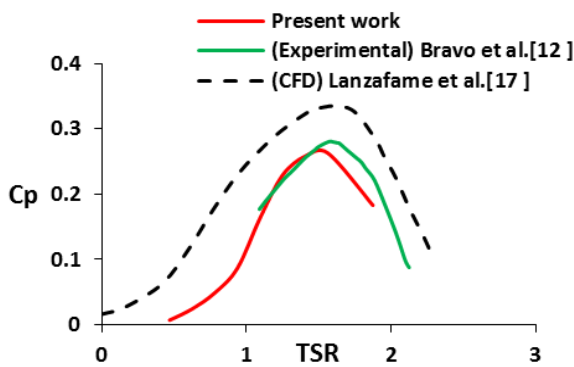


Figure 4. Validation curve between present CFD with experimental data [12] and another numerical data [17]

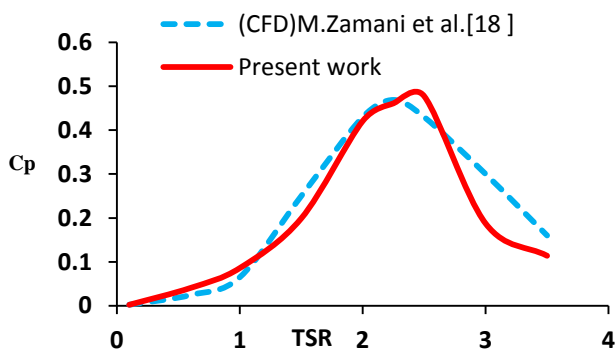


Figure 5. Verification curves that Compare between the present numerical model and another computational results for Darrieus rotor [18].

A double check on convergence is applied; the first convergence criterion is depending on the torque coefficient C_m . The global convergence criterion, each simulation ends when the variation between the values of the torque coefficient C_m shows a deviation of less than 1% compared with equivalent values of the previous periods. As shown in Fig.6 about 15 revolutions have been achieved the quasi-steady state is obtained at revolution 7. The second check is performed on the residuals that must be less than 10^{-5} for each physical time step. The power coefficient C_p and the torque coefficient C_m are calculated by averaging the results during the last three cycles. The calculations performed on 8 thread processors, 3.40 GHz clock frequency PC. The time step is calculated at each angular velocity for marching angular step 1° that is recommended by Trivellato and Castelli [19] especially at small tip speed ratios and sensitive spatial discretization schemes. Equation (6) pointed out that power generated is proportional to the cubed wind speed; any acceleration in the speed of wind that hits the wind turbine will directly improve the output power. Ghazalla et al. [20] described all wind lens dimensions in details see Fig.7 and stated that the optimum location for wind lens was $X/D=-0.3$ with respect to wind turbine that is installed at the origin (0, 0). The scope of the present work is to study the effect of J-cut at different designs using S1046 aerofoil on performance

enhancement followed by aero-acoustic investigation. Ref [20]&[21] confirmed that the appropriate operating conditions for J-cut design were at low tip speed ratios ($\lambda < 2$) and high solidity.

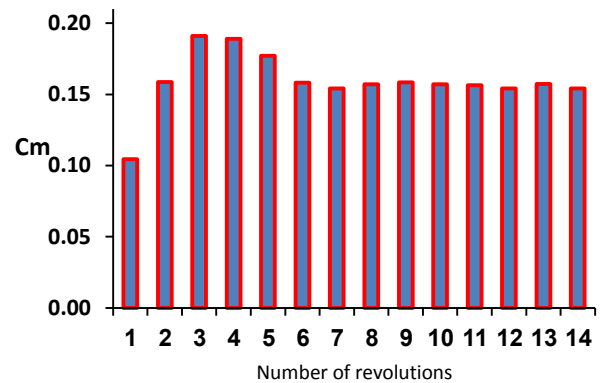


Figure 6. Torque coefficient convergence history over more 14 revolutions at $\lambda=1.6$

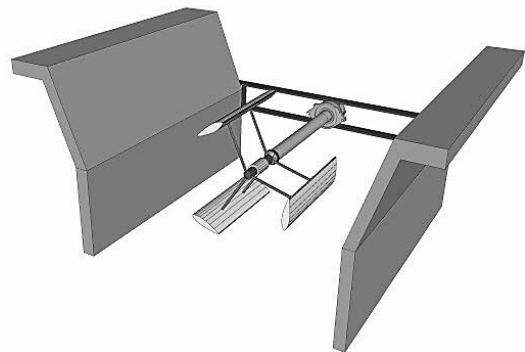


Figure 7. Darrieus turbine enclosed by wind lens

A. Aeroacoustic prediction model settings

The noise generated from Darrieus turbine can be calculated using Lighthill and Ffowcs Williams-Hawkings. Lighthill's used a nonhomogeneous sound wave equation for the sound pressure p' Eq. (7)

$$\frac{1}{c^2} \frac{\partial^2 p'}{\partial t^2} - \frac{\partial p'}{\partial x_i^2} = \frac{\partial^2 T_{ij}}{\partial x_i \partial x_j} \quad (7)$$

left hand indicated the homogenous wave equation while the tensor T_{ij} was considered as a source term derived by Lighthill. It is derived from the conservation of mass and momentum as shown in Eq. (8):

$$T_{ij} = P_{ij} + \rho u_i u_j - c^2 \delta_{ij} \rho' = \rho u_i u_j + (p - c^2 \rho') \delta_{ij} - \tau_{ij} \quad (8)$$

$\rho u_i u_j$, non-linear convective forces, $c^2 (p - c^2 \rho')$ is the sound speed deviations

$$T_{ij} = \rho u_i u_j \quad (9)$$

T_{ij} are the forces of viscosity, u_i is fluid velocity component in the x_i direction and the Kronecker delta δ_{ij} . A non-linear convective effects $\rho u_i u_j$ remain as sound sources and Eq. (8) was simply became as follow:

Eq. (7) is multiplied by function w , then integrated on the computational domain Ω and finally Stokes-integral theorem is applied.

$$\int_{\Omega} \frac{1}{c^2} \frac{\partial^2 p'}{\partial t^2} w d\Omega + \int_{\Omega} \frac{\partial w}{\partial x_i} \frac{\partial p'}{\partial x_i} d\Omega - \int_{\Gamma} \frac{\partial p'}{\partial n} w d\Gamma - \int_{\Omega} \frac{\partial w}{\partial x_i} \frac{\partial T_{ij}}{\partial x_j} d\Omega \quad (10)$$

The free space Green's function is applied as illustrated in Eq. (11) to obtain the radiation into free field:

$$G(x, t) = \frac{\delta(t - |x_i - y_i| - \tau/c_0)}{4\pi|x_i - y_i|} \quad (11)$$

Where c_0 the ambient speed of the sound and the delayed time is τ . The formula of Farassat [22] inside SPySI (Surface Prediction by Surface Integration) is used. For a static porous integration surface S , it is solved as follows:

$$p'(x, t) = p'_Q(x, t) + p'_L(x, t) + p'_T(x, t) \quad (12)$$

As the p'_T is the thickness of the noise. It describes the physical component of the fluid in the flow field by solid surfaces such as turbine blades. The loading noise term p'_L represents the physical component of the force that acts on the fluid as a result of the nearness of the surfaces. The "quadrupole-distribution" is described by p'_Q . By ignoring the volume forces then integrate on the surface S , the noise thickness and loading of the noise are calculated as follows:

$$4\pi p'_T(x, t) = \frac{\partial}{\partial t} \int_S \left[\frac{\rho_0 U_n}{r} \right]_{ret} dS \quad (13)$$

$$4\pi p'_L(x, t) = \frac{1}{c_0} \frac{\partial}{\partial t} \int_S \left[\frac{L_r}{r} \right]_{ret} dS + \int_S \left[\frac{L_r}{r^2} \right]_{ret} dS \quad (14)$$

The linear distance between the source and the receiver location is represented by r and sub-script n is the scalar contraction with the integration surface normal vector n_i .

The variables U_i and L_i are presented by Di Francescantonio [23] as following:

$$U_i = \frac{\rho}{\rho_0} u_{ij}, \quad L_i = P_{ij} n_j + \rho u_i \quad (15)$$

The proposed algorithms to solve the wave propagation time between source and observer namely the "advanced time" method using Eq.16. The acoustic analysis is needed 1 time step for each CFD simulation.

$$t_{adv} = t + \frac{r(t)}{c_0} \quad (16)$$

Four receivers are located at different positions that is considered source data collector to predict the aero-acoustics noise see Fig.8. The signals are obtained via Ffowcs Williams-Hawkings acoustic model at the last revolution. Using FFT in fluent was to convert the time independent data from transient solution to frequency measured in hertz. The sound pressure level (SPL) is computed then represented to provide accurate predictions about noise propagations emanated from different designs that will be discussed in details at the next section.

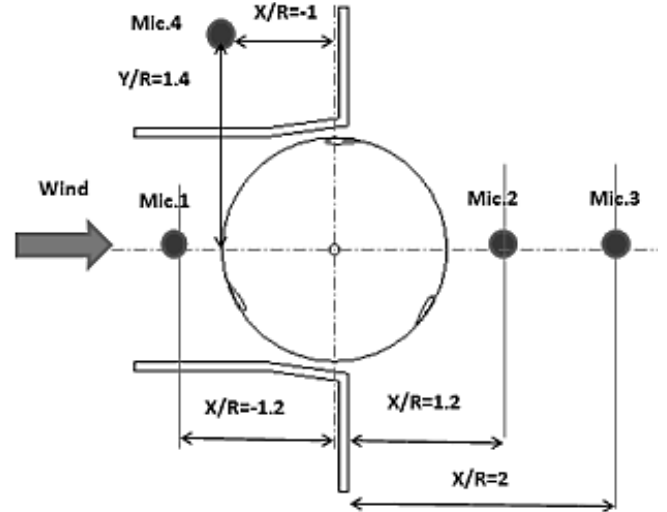


Figure 8. The receivers locations placed at Darrieus turbine equipped with wind lens.

III. RESULTS AND DISCUSSION

This section deals with studying the effect of J-cut profile with and without the wind-lens on the performance and the noise generation. Four different designs are tested using 3-blades of S1046 symmetric aerofoil type. They are as follows:

1. The original profile of S1046 placed without wind-lens (open) in Darrieus turbine.
2. The original profile enclosed by wind lens.
3. The modified aerofoil (J-cut) placed without wind-lens in Darrieus turbine.
4. The modified aerofoil (J-cut) enclosed by wind lens.

It reveals from the results that J-cut without the diffuser has better effect on power coefficient compared with open turbine only at all tip speed ratios. The S1046 aerofoil is enhanced the power augmentation factor by 1.74 in second design (open turbine + wind lens) and in case of fourth design (J-cut with wind lens) the power augmentation factor was 1.348 Fig.9. The flanged wind lens has significant role in accelerating, collecting and directing the wind through Darrieus rotor. Figure11 showed pressure contours, velocity contours of S1046 open turbine and with wind lens respectively. It is cleared from cyan and greenish yellow color that the wind velocity near the blades increased to 20 m/s in case of flanged wind lens that is lacked by open turbine.

Accordingly it is concluded that the most efficient designs are original profile shape and J-cut enclosed by wind lens all over the remaining designs. Hence it is important to investigate another parameter that is considered as the main disadvantage of Darrieus turbine. Namely static torque coefficient that is mainly responsible for self-starting capability of VAWT. Self-start (starting torque) is investigated using steady state simulations to obtain the static torque coefficient.

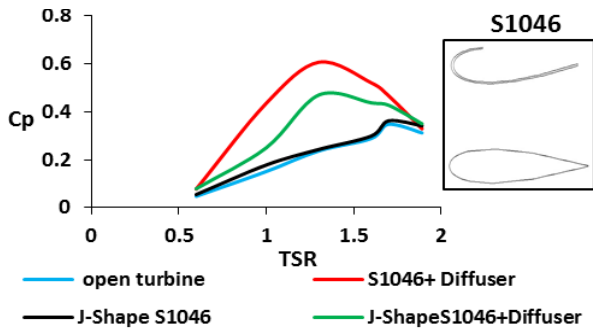


Figure 9. Power coefficient values obtained from 4 different configurations at different TSRs

In Fig.10 the self-start capability of S1046 is investigated with wind lens using both original and J-cut profile. It is cleared that the static torque coefficient of J-cut shape of S1046+diffuser has less self-starting capability by 0.297 times the static torque coefficient obtained from the original shape of S1046+wind lens.

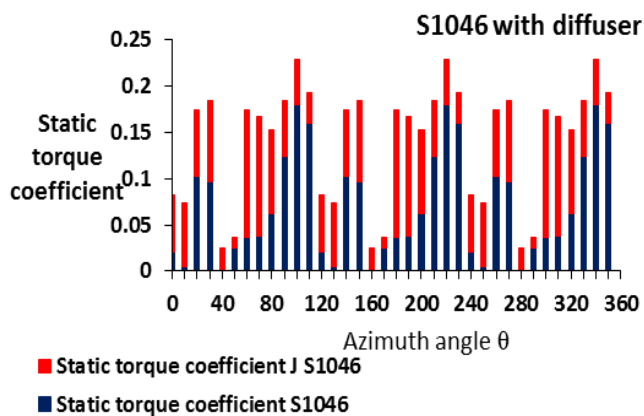


Figure 10. Static torque coefficient for conventional shape and j shape of S1046 with wind lens.

A. Aeroacoustic results

The Aero-acoustic results is computationally investigated and represented by plotting sound pressure level SPL measured in (dB) against the frequency in (Hz) known as spectral analysis. The SPL can be defined as $SPL = 20 \log_{10} \left(\frac{P}{P_{ref}} \right) dB$ where, P_{ref} is the reference pressure in air (10^{-5}). The noise generated from Darrieus turbine is obtained using Fast Fourier Transform at the optimum tip speed ratios that belong to each design. A bare wind turbine and three remaining designs are investigated from aero-acoustic point of view. In Fig.12 the J-cut profile without wind lens for S1046 revealed that is the least noise intensity emitter design compared to the other designs as illustrated. The new J-cut profile wind turbine augmented with wind lens is recorded the noisiest design at the optimum TSRs and at different microphones locations. In addition, changing TSR from $\lambda=1.3$ to $\lambda=1.7$ does not

extremely affect the noise level for all designs. It is noted that the new J-cut without wind lens produces an overall averaged sound pressure level (OASPL) of 55.3 dB that can play an important role in the noise reduction point of view. The acoustic prediction for all the configurations shows significant effect for J cut paradigm on decreasing the noise level after 2500Hz.

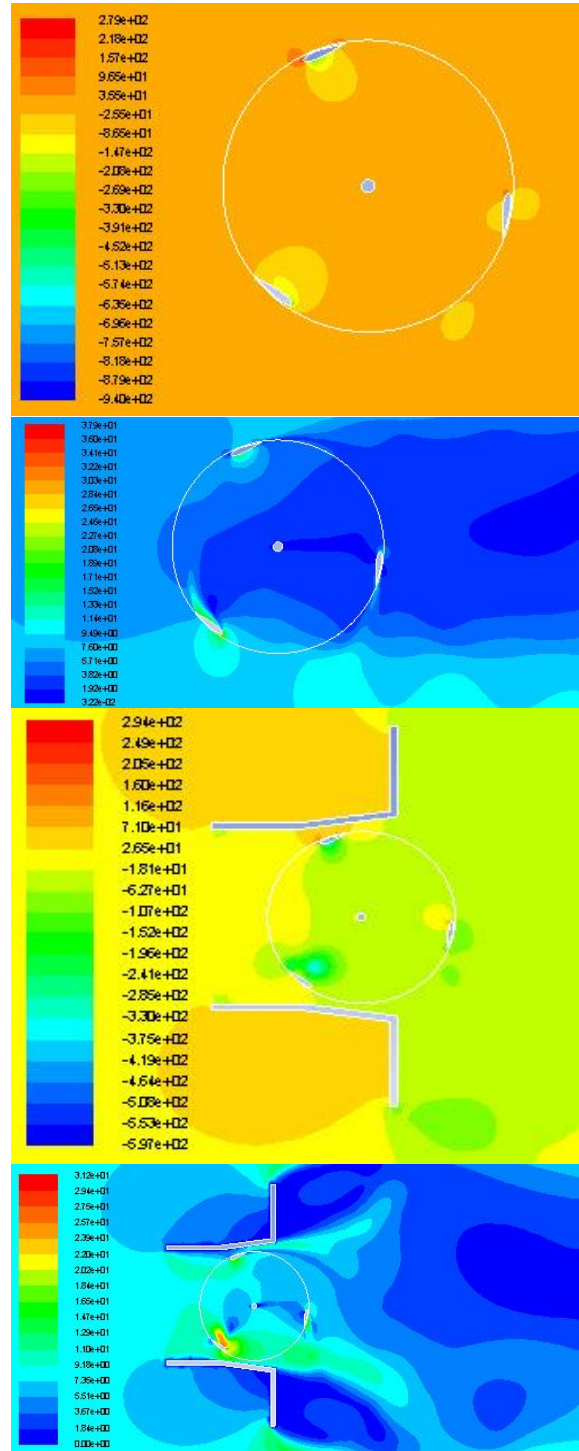


Figure 11. Pressure and velocity contours for S1046

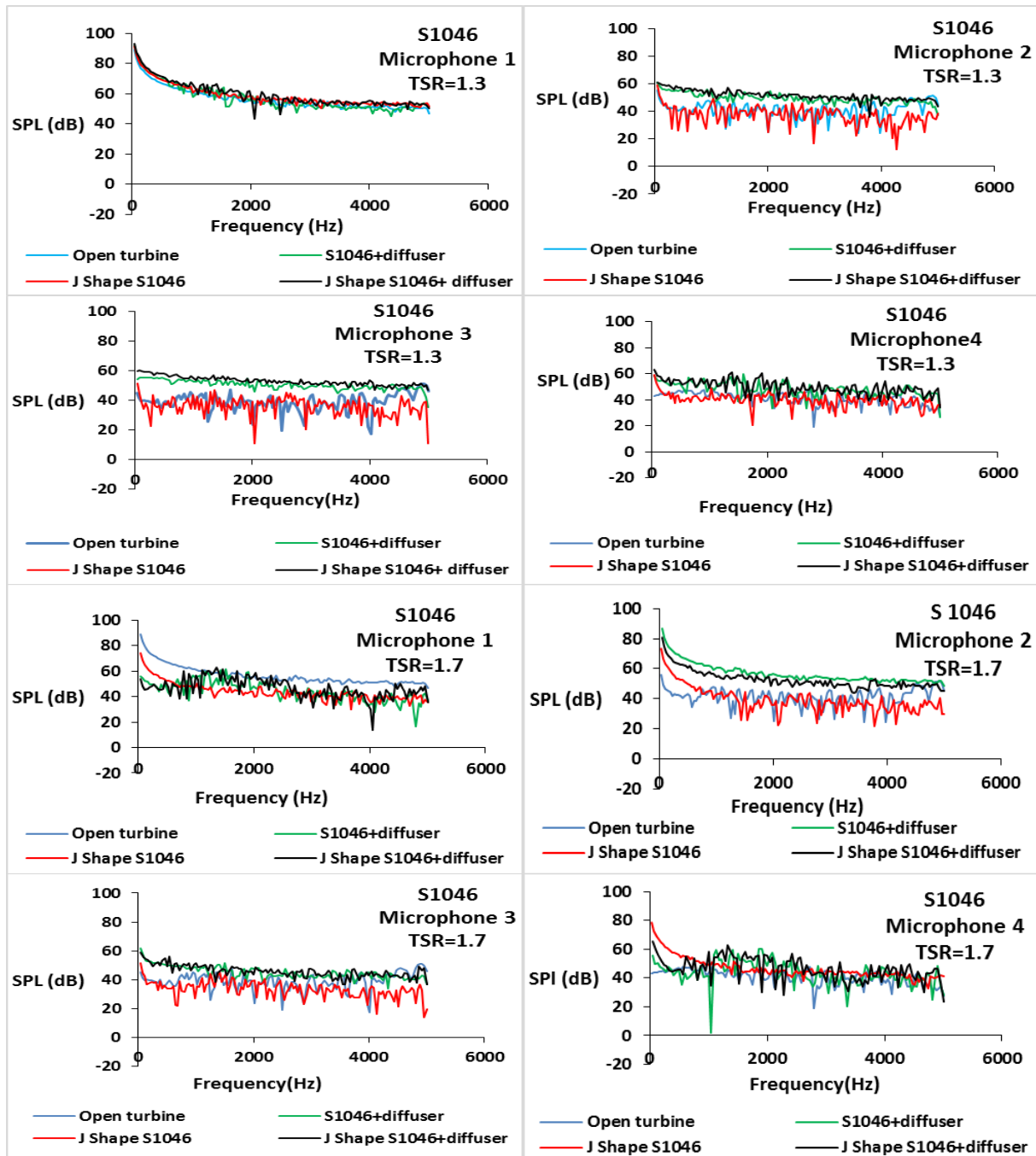


Figure 12. SPL (dB) Vs. frequency in (Hz) for S-1046 aerofoil for all the 4 designs

IV. CONCLUSION

The present work aims to increase the aerodynamic performance of the Darrieus rotor without increasing the noise pollution. These objectives were achieved by using wind lens and new J-cut for the original aerofoils. The investigation is performed using 3 blades of S1046 aerofoil operated at constant wind speed= 8m/s at low speed tip ratios and high solidity the results revealed that:

- The open turbine with the new J-cut profile of S1046 has a significant effect on enhancement of generated power at all tip speed ratios.
- The wind lens with flange helped in capturing and accelerated the flow quickly through the Darrieus turbine.
- The power coefficient is enhanced by a factor of 1.74 in case of original S1046 aerofoil enclosed in wind lens and in case of the new J-cut with wind lens the power augmentation factor was 1.348.

- The new J-cut shape of S1046+wind lens has less self-stating capability by 0.297 times the static torque coefficient obtained from the original shape of S1046+wind lens.
- The new J-cut profile without wind lens for S1046 revealed that is the least noise intensity emitter design compared to the other 3 designs.
- The wind lens improved the produced power but has but also increased the noise.
- The new J-cut without wind lens produces an overall averaged sound pressure level (OASPL) of 55.3 dB
- The new J-cut profile is promising from performance and aeroacoutics point of view but at the high solidity and low tip speed ratios ($\lambda < 2$) for Darrieus turbine.

NOMENCLATURE

A: Projected area of rotor [m^2]
 Cm: Torque coefficient [-]
 Cp: Power coefficient [-]
 C: Blade chord length [m]
 D: Throat width [m]
 H: Flange width [m]
 h: Rotor height [m]
 k: Turbulence kinetic energy [J/kg]
 L: Diffuser length [m]
 L_t : Total diffuser length [m]
 N: Number of blades [-]
 P: Mechanical power [W]
 R: Rotor radius [m]
 S: Clearance [m]
 T: Mechanical torque [N.m]
 U: Blade speed [m/s]
 U ∞ : Wind speed [m/s]
 y⁺: Normalized wall distance [-]

Greek symbols

ϵ : Turbulence dissipation rate [J/kg.s]
 λ : Tip-speed ratio [-]
 μ : Dynamic viscosity [kg/m.s]
 ν : Turbulence kinematic viscosity [m^2/s]
 θ : Azimuth angle [$^\circ$]
 ρ : Density [kg/m^3]
 σ : Rotor solidity [-]
 φ : Diffuser semi-open angle [$^\circ$]
 ω : Angular velocity [rad/s]

Abbreviations

CFD: Computational Fluid Dynamics
 FFT: Fast Fourier Transform
 FVM: Finite Volume Method
 HAWT: Horizontal Axis Wind Turbine
 NACA: National Advisory Committee for Aeronautics
 OSPL: Overall Sound Pressure Level
 SIMPLE: Semi-Implicit Method for Pressure-Linked Equations

SMM: Sliding Mesh Model

URANS: Unsteady Reynolds Averaged Navier-Stokes

VAWT: Vertical Axis Wind Turbine

REFERENCE

- [1] Howell, Robert, Ning Qin, Jonathan Edwards, and Naveed Durrani. "Wind tunnel and numerical study of a small vertical axis wind turbine." *Renewable Energy* 35 (2010): 412-422.
- [2] Beri, H., and Y. Yao. "Effect of Camber Airfoil on Self-starting of Vertical Axis Wind Turbine." *Journal of Environmental Science and Technology* 4-3 (2011): 302-312.
- [3] Raciti Castelli M, Englaro A, Benini E. The Darrieus wind turbine: proposal for a new performance prediction model based on CFD. *Energy* 2011; 36:4919-34
- [4] Wakui, Tetsuya, Yoshiaki Tanzawa, Takumi Hashizume, and Toshio Nagao. "Hybrid Configuration of Darrieus and Savonius Rotors for Stand-Alone Wind Turbine- Generator systems. *Electr Eng Jpn* 2005; 150(4):13-22.
- [5] Gupta, R., R. Das, R. Gautam, and S.S. Deka. "CFD Analysis of a Two bucket Savonius Rotor for Various Overlap Conditions." *ISESCO Journal of Science and Technology* 8-13 (May 2012): 67-74.
- [6] C. Consult, R. Willden, E. Ferrer, M.D McCulloch, Influence of solidity on the performance of a cross-flow 467 turbine, 8th European wave and Tidal Energy Conference (2009) Systems." *Electrical Engineering in Japan* 150-4 (2005): 259–266.
- [7] Mohamed MH. "Performance investigation of H-rotor Darrieus turbine with new airfoil shapes." *Energy* 47 (2012): 522-530.
- [8] Kanyako F, Janajreh I. "Numerical investigation of four commonly used airfoils for vertical Axis wind turbine." In: *ICREGA'14-Renewable Energy Gener. Appl. Springer Proc. Energy*; 2014
- [9] Watanabe K, Takahashi S, Ohya Y. "Application of a diffuser structure to vertical-axis wind turbines." *Energies* 2016; 9.
- [10] Ohya Y, Karasudani T, Sakurai A, Abe KI, Inoue M. Development of a shrouded wind turbine with a flanged diffuser. "*J Wind Eng Ind Aerodyn* 2008; 96: 524-539.
- [11] I.Hashem and M.H.Mohamed, Aerodynamic performance enhancements of H-rotor Darrieus wind turbine. *Energy* 142 (2018): 531-545.
- [12] R. Bravo, S. Tullis, S. Ziada, Performance testing of a small vertical-axis wind turbine, in: *Proceedings of the 21st Canadian Congress of Applied Mechanics (CANCAM07)*, Toronto, Canada, June 2007; 3-7.
- [13] A. Iida, A. Mizuno and K. Fukudome, Numerical Simulation of Aerodynamic Noise Radiated from Vertical Axis Wind Turbines, Technical Report, Kogakuin University Department of Mechanical Engineering, 2004
- [14] C. Pearson and W. Graham, Investigation of the noise sources on a vertical axis wind turbine using an acoustic array, 19th AIAA/CEAS Aeroacoustics Conference, Berlin, 2013
- [15] Mohamed MH, Aeroacoustics noise evaluation of H-rotor Darrieus wind turbines, *Energy*, 65, 2014, 596-604
- [16] Mohamed MH, Ali AM, Hafiz, CFD analysis for H-rotor Darrieus turbine as a low speed wind energy converter. *Eng Sci Technol Int J* 2015.
- [17] R. Lanzafame, S. Mauro, M. Messina, "2D CFD modeling of H-Darrieus wind turbines using a transition turbulence model," *Energy Proced.* 45 (2014) 131e140.
- [18] Zamani M, Maghrebi MJ, Varedi SR, Starting torque improvement using J-shaped straight-bladed Darrieus vertical axis wind turbine by means of numerical simulations. *Renew Energy* 2016; 95:109-26.
- [19] Trivellato F, Raciti Castelli M. On the Courant-Friedrichs-Lewy criterion of rotating grids in 2D vertical-axis wind turbine analysis. *Renew Energy* 2014;62:53.
- [20] Ghazalla RA, Mohamed MH, Hafiz AA. CFD Assessment of Darrieus Turbine performance under different parameters, vol. 13. Cairo, Egypt: ICFD; December 2018. pp. 1-12.

- [21] M.H. Mohamed, Criticism study of J-Shaped darrieus wind turbine: Performance evaluation and noise generation assessment, *Energy* (2019) 367-385
- [22] F. Farassat, Introduction to generalized functions with applications in aerodynamics and aeroacoustics, Technical Report, 1996, NASA
- [23] P. Di Francescantonio, A New Boundary Integral Formulation for the Prediction of Sound Radiation, *Journal Sound and Vibration*, Vol.202, No. 4, 1997, pp. 491–509

How to Cite this Article:

Ghazalla, R. A., Mohamed, M. H. & Hafiz, A. A. (2019) Numerical Study for Darrieus Turbine with Wind Lens: Performance and Aeroacoustic Analogies. *International Journal of Science and Engineering Investigations (IJSEI)*, 8(88), 74-83. <http://www.ijsei.com/papers/ijsei-88819-14.pdf>

